How Counting Statistics Controls Detection Limits and Peak Precision

D. A. Gedcke

When Counting Statistics Dominates

For spectrometers that measure and count individual events, such as those listed in Table 1, counting statistics normally controls the precision for measuring the number of events. In the case of a small peak superimposed on a high background in the acquired spectrum, the fluctuation in the background counts seriously degrades the precision with which the net peak counts can be measured. Ultimately, it is this uncertainty in the background counts that determines the detection limit for the peak.

Table 1. Typical Particles and Photons Associated with Counting Statistics

Ionized molecules	Neutrons
Molecules	Electrons
Ions (atomic or molecular)	Beta particles
Atomic nuclei	Gamma rays
Alpha particles	X rays
Protons	IR to UV photons

This application note examines the contribution of counting statistics to the uncertainty in determining the net peak area, and in controlling detection limits. The methodology is applicable to spectrometers that count single events. (See examples in Table 2.) The results show that it is important to maximize the peak-to-background ratio, the event counting rate, and the counting time. The latter two parameters improve precision by increasing the number of measured counts.

Table 2. Spectrometers Dominated by Counting Statistics

- Time Digitizers used in Time-of-Flight Mass Spectrometry (TOF-MS)
- Time Digitizers or Multichannel Scalers (MCS) responding to single photons in LIDAR, or fluorescence and phosphorescence lifetime spectrometry
- Time-of-flight spectrometry with nuclear radiation (neutrons, alpha and beta particles, ions and nuclei)
- Pulse-amplitude or energy spectrometry with nuclear radiation (gamma-rays, X-rays, alpha particles, recoiling nuclei) using multichannel analyzers (MCA)
- Time spectrometry using a time-to-amplitude converter (TAC) followed by an MCA

Poisson Statistics Applies

The above applications normally meet the conditions that define the Poisson Distribution[1, 2]:

1) The events are uniformly and randomly distributed over the sampling intervals.
2) The probability of detecting an event during an infinitesimal time interval dt is ρdt, where ρ is the expected counting rate.
3) $\rho dt \ll 1$.
4) The probability of detecting more than one event during the infinitesimal time interval dt is negligible.

If the events are counted over a finite time period, t, the Poisson Distribution, P(N), describes the probability of recording N counts in a single measurement of duration, t.

$$P(N) = \frac{\mu^N e^{-\mu}}{N!} \qquad (1)$$

If the measurement is repeated a large number of times and the values of N are averaged, the average value of N approaches the mean of the distribution, μ, as the number of repeated measurements approaches infinity. Note that the Poisson Distribution has a standard deviation

$$\sigma_N = \sqrt{\mu} \approx \sqrt{N} \qquad (2)$$

Substituting N for μ in equation (2) recognizes that the value of N from a single measurement is an adequately accurate estimate[1] of μ.

A more useful description of the precision of the measurement is obtained by multiplying the relative standard deviation, σ_N / N, by 100% to express the percent standard deviation as

$$\sigma_N\ \% = \frac{\sigma_N}{N}\ x\ 100\% = \frac{100\%}{\sqrt{N}} \qquad (3)$$

Table 3 shows how the percent standard deviation improves as the counted number of events increases.

Clearly, a large number of events must be accumulated to achieve a precision better than 1%.

Table 3. σ_N% for Selected Values of N.

N	σ_N%
1	100.0%
100	10.0%
10,000	1.0%
1,000,000	0.1%

Strictly speaking, equations (1) through (3) accurately describe the statistical distribution of events counted only if a) dead time losses are negligible, or b) if an ideal livetime clock is employed to compensate for dead time losses[3-8]. For the purpose of this application note, at least one of these conditions will be presumed to be satisfied.

Optimum Precision for a Peak with Zero Background

Most of the spectrometers in Table 2 produce spectra composed of widely separated peaks sitting on a slowly varying background. The position of the peak along the horizontal axis represents the main parameter to be measured. This may represent the flight time of the particles or photons in a time-of-flight spectrometer, the mass of the particles in mass spectrometry, or the energy of the particles or photons in pulse-height spectrometry. The centroid of the peak is typically used to mark the peak position and to provide an accurate measure of the flight time, mass, or energy in the above examples. The area of the peak measures the probability of detecting events with that specific flight time, mass, or energy. A Gaussian peak shape is normally a good approximation to the actual shape of the peaks in the spectrum. Consequently, it will be used as a pragmatic model for investigating methods for extracting the optimum information from the spectrum.

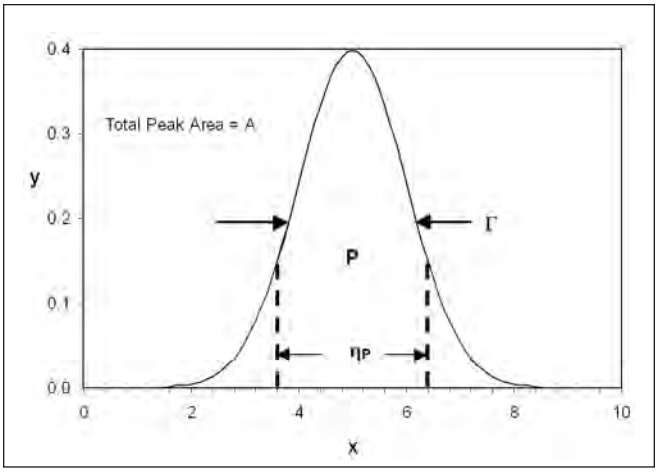

Figure 1. Integrating the counts in a selected region of a Gaussian peak.

The special case of zero background is instructive for learning how to extract all the information from the peak in the more general case of non-zero background. Therefore, consider the Gaussian peak in Figure 1. The y axis represents the number of events counted per unit interval on the x axis. The Full Width at Half Maximum height (FWHM) of the peak is Γ. The dashed lines, located an equal distance to the right and left of the centroid, define the region of the peak from which the counts will be extracted. The width of this region is η_P, and the total number of counts defined by the area of this region is P. The number of events counted in the entire peak is denoted by A, the total area of the peak.

If the counts from entire area of the peak are summed, the relative standard deviation in those counts is

$$\frac{\sigma_A}{A} = \frac{1}{\sqrt{A}} \qquad (4)$$

This is the best precision available from the peak, because A is the largest number of counts that can be extracted from the peak. The integration region of width η_P uses less than the full number of events counted in the peak, and yields a relative standard deviation given by

$$\frac{\sigma_P}{P} = \frac{1}{\sqrt{P}} \qquad (5)$$

It is useful to compare the precision obtained in equation (5) with the best precision that is achievable by dividing equation (5) by equation (4).

$$\frac{\sigma_P / P}{\sigma_A / A} = \frac{\sigma_P}{P}\sqrt{A} = \frac{\sqrt{A}}{\sqrt{P}} \qquad (6)$$

Equation (6) is plotted in Figure 2 versus the ratio of the width of the integration region to the FWHM of the peak. The horizontal dashed line in Figure 2 represents the best precision that can be achieved when the entire area of the peak is integrated. For narrower integration regions the precision degrades, and the degradation escalates rapidly as the width of the integration region approaches zero.

It is obvious from Figure 2, that the width of the integration region should be wider than twice the FWHM of the peak, in order to achieve the best precision. The condition, $\eta_P = 2\ \Gamma$ integrates 98% of the events counted in the peak. Where possible, an even wider integration region is advisable to avoid errors caused by inadvertent misalignment of the integration window relative to the centroid of the peak. Misalignment can arise from peak shifts caused by changes in counting rate or temperature. If the centroid of the peak is calculated by the standard centroid algorithm[9], an integration region wider than 2 Γ is critical for avoiding misalignment errors in the computed peak position. If the entire area of the peak is used to calculate the centroid, ORTEC Application Note AN58 shows that the random error caused by counting statistics is[9, 13]

$$\sigma_c = \frac{\Gamma}{2.35\sqrt{A}} \qquad (7)$$

where σ_c is the standard deviation in the x coordinate for the centroid of the peak. If the entire peak cannot be used to extract the centroid information, a least squares fit of the known peak shape to the central portion of the peak can be productive for finding the peak position with reasonable accuracy[2, 10, 11, 12]. This same technique can be used to minimize misalignment errors when determining the total area of the peak. For pedagogic simplicity, this application note will presume a simple integration of the counts is used as depicted in Figure 1. The random error that controls precision and detection limits is similar for both methods, i.e., least squares fitting or simple integration.

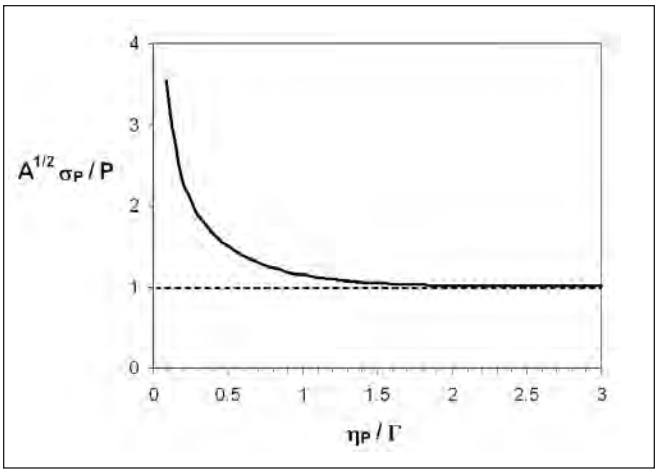

Figure 2. The figure of merit for precision in the peak counts versus the width of the integration region, η_P.

Detection Limits with Zero Background

Detection limits for a peak are typically defined by setting a threshold that the counts in the peak must exceed to claim detection. The threshold is chosen so that there is a 95% probability of the counts exceeding that threshold if the peak is truly present in the spectrum. That defines the 95%-confidence limit. This choice implies that there is a 5% probability of not detecting the peak, even though it is truly present.

With zero background a single count is the minimum that can be detected. From equation (1) we seek the value of μ for which there is a 95% probability that the value of N will exceed zero in a single measurement. This is identical to finding the value of μ for which there is a 5% probability of recording zero counts in a single measurement. That probability is expressed in equation (8) and set equal to 0.05 to find the value of μ corresponding to the detection limit.

$$P(0) = \frac{\mu^0 e^{-\mu}}{(0)!} = e^{-\mu} = 0.05 \qquad (8)$$

The solution is

$$\mu = -\ln(0.05) = 3.00 \qquad (9)$$

Thus a detection threshold set at N ≥ 1 provides a 95%-confidence detection limit at

$$A_{DL0} = 3 \text{ counts} \qquad (10)$$

Typically the counts in the peak are related to the concentration C for the component of the material being measured by a calibration constant k.

$$C = k\,A \qquad (11)$$

This leads to the specification of the minimum detectable concentration for the case of zero background:

$$C_{DL0} = k\,A_{DL0} = 3\,k \qquad (12)$$

In mass spectrometry C represents the concentration of the molecule of mass m in the original sample. For radioactive nuclide spectrometry, C is the activity of the specific radioisotope.

If a first attempt at the measurement yields detection limits that are not low enough, what can be done to improve the detection limit? The simplest solution is to increase the counting time. For the special case of zero background, doubling the counting time will double A and decrease k by a factor of 2 in equation (11). This lowers C_{DL0} by a factor of 2 in equation (12). In other words, detection limits are

lowered by decreasing the concentration required to yield an average of 3 counts. This can be accomplished by a) increasing the counting time, and/or b) improving the yield of counts per unit concentration from the sample. Solution b) could involve improving the efficiency of the measurement apparatus, or pre-concentration of the desired component in the sample.

A Gaussian Approximation for the Poisson Distribution

Moving to the general case of a peak sitting on a background requires subtraction of the background to determine the net peak counts. As is revealed below, this requires development of the Gaussian approximation to a Poisson distribution so that the random error in the net peak counts can be calculated.

If the counts from two separate measurements are added to form a sum

$$N_+ = N_1 + N_2 \tag{13}$$

and N_1 and N_2 are both defined by their own Poisson distributions, then N_+ also has a Poisson distribution defined by[1]

$$P(N_+) = \frac{\mu_+^{N+}\, e^{-\mu+}}{N_+!} \tag{14}$$

where μ_+ is the sum of the means from the two distributions, as well as the mean for the distribution of the sum.

$$\mu_+ = \mu_1 + \mu_2 \tag{15}$$

This relationship makes it easy to compute the standard deviation of the sum from

$$\sigma_{N+} = \sqrt{\mu_+} \approx \sqrt{N_+} = \sqrt{N_1 + N_2} \tag{16}$$

Unfortunately, no such simple relationship exists for the difference of two counts

$$N_- = N_1 - N_2 \tag{17}$$

because the difference no longer follows a Poisson distribution[1]. In this case, one has to resort to the Gaussian approximation to a Poisson distribution.

Figure 3 shows how the shape of the Poisson distribution changes as its mean value, μ, increases. For values of μ approaching 1, the distribution is notably asymmetric. As μ increases, the distribution becomes more symmetric, and begins to resemble a Gaussian shape. Figure 4 compares Poisson distributions for μ = 9 and μ = 36 to the Gaussian probability distribution

$$G(N) = \frac{e^{-\frac{(N-\mu)^2}{2\sigma^2}}}{\sqrt{2\pi\sigma^2}} \tag{18}$$

where the special condition

$$\sigma^2 = \mu \tag{19}$$

has been inserted in equation (18) to make the mean and standard deviation for the Gaussian curve match the mean and standard deviation of the Poisson distribution. The correspondence between the two distribution types is surprisingly good for a value of m as low as 9. For the purposes of computing and combining standard deviations, the Gaussian distribution is an adequate approximation to the Poisson probability distribution for μ ≥ 9.

The Gaussian probability distribution fulfills equations (13), (15), and (16) for the distribution of the sum of counts from two Gaussian distributions. In fact, the distribution of N_+ is also a Gaussian function. Furthermore, the distribution of the difference of two counts

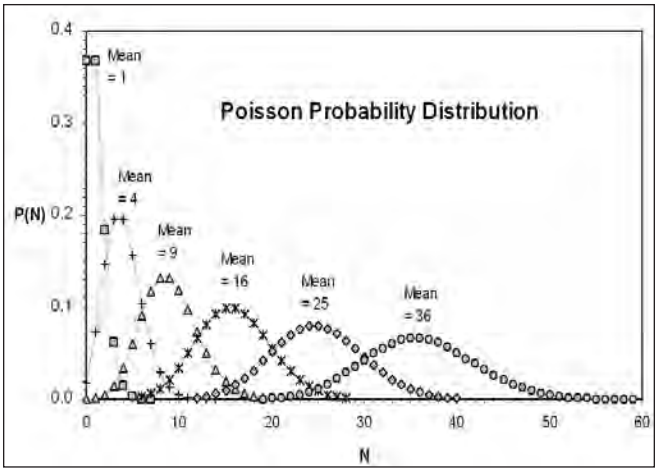

Figure 3. The Poisson probability distribution for various values of the mean, μ.

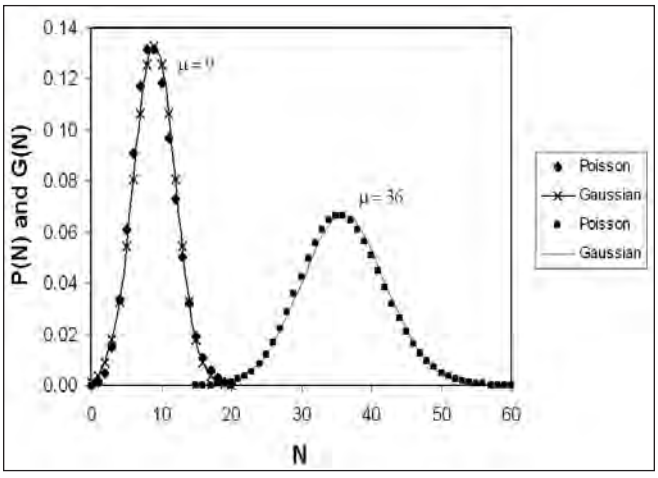

Figure 4. A comparison between the Poisson and Gaussian distributions for $\mu = \sigma^2 = 9$ and $\mu = \sigma^2 = 36$. The Poisson distributions are represented by the solid diamonds and squares, while the Gaussian distributions are plotted as continuous lines.

$$N_{-} = N_1 - N_2 \quad (17)$$

has a Gaussian distribution, if the distributions of N_1 and N_2 are both Gaussian[1]. The mean of the distribution for N_{-} is

$$\mu_{-} = \mu_1 - \mu_2 \quad (20)$$

But, the standard deviation for N_{-} is

$$\sigma_{N-} = \sqrt{\sigma_1^2 + \sigma_2^2} \approx \sqrt{N_1 + N_2} \quad (21)$$

Note the crucial "+" signs in equation (21) in spite of the "–" signs in equations (17) and (20). The results surrounding equations (20) and (21) stem from the shape and symmetry of the Gaussian function.

The calculations in the next section require one more principle for deriving standard deviations from functions incorporating Gaussian probability distributions. If N is distributed according to a Gaussian probability function and β is a constant, then

$$M = \beta N \quad (22)$$

also has a Gaussian distribution with a standard deviation[1, 2]

$$\sigma_M = \beta\sigma_N \quad (23)$$

where σ_N is the standard deviation of the probability distribution for N.

The equations summarized above for the Gaussian approximation are the tools needed for calculating the precision of the net peak counts for a peak sitting on a background.

Peak Precision in the Presence of Background

Figure 5 illustrates a simple method for subtracting the background lying under a peak to extract the net peak counts. This is a practical algorithm whenever the background varies slowly enough in the vicinity of the peak to be approximated by a straight line spanning the location of the peak. A region of interest (ROI) of width η_P is marked on the peak, and the counts in that region are integrated. The total integrated area, N_T includes the background counts, B, as well as the net peak counts, P.

$$N_T = P + B \quad (24)$$

To estimate B, two additional regions of interest are integrated, one a distance d to the left of the peak ROI, and another a distance d to the right of the peak ROI. The widths of both of these background regions are set equal ($\eta_B/2$). The counts integrated from the left background region are designated N_{B1}, while the counts summed in the right background region are denoted N_{B2}. Consequently, the estimate of the background included under the peak becomes

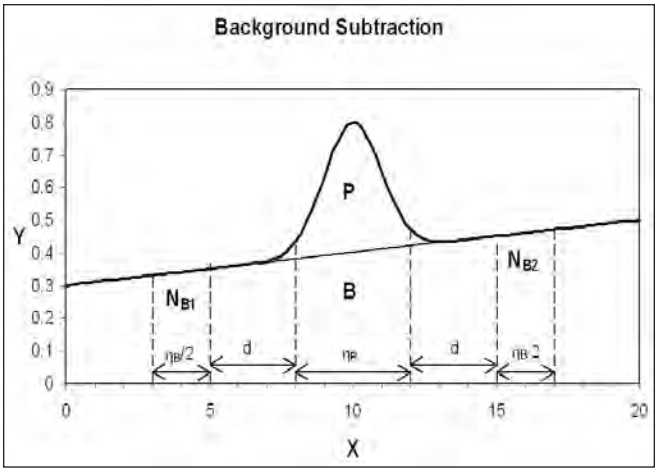

Figure 5. A simple method for background subtraction.

$$M_B = \frac{\eta_P}{\eta_B}(N_{B1} + N_{B2}) \approx B \quad (25)$$

with a standard deviation

$$\sigma_{MB} \approx \frac{\eta_P}{\eta_B}\sqrt{N_{B1} + N_{B2}} \approx \frac{\eta_P}{\eta_B}\sqrt{\frac{\eta_P}{\eta_B}B} \quad (26)$$

Therefore, the net peak counts can be estimated by subtracting the background estimate via equation (27).

$$P \approx N_T - M_B \quad (27)$$

The standard deviation in this estimate of the net peak counts is

$$\sigma_P = \sqrt{\sigma_{NT}^2 + \sigma_{MB}^2} \quad (28)$$

which simplifies to

$$\sigma_P \approx \sqrt{P + \left(1 + \frac{\eta_P}{\eta_B}\right) B} \qquad (29)$$

The first term, P, under the square root sign is the contribution the peak counts would make to the precision if there were no background, i.e., when B = 0. The second term is the degradation of the precision caused by the background. Note that the background contribution is amplified by the factor in the parentheses.

Following the principle defined in equation (6), the figure of merit for equation (29) can be expressed as

$$\frac{\sigma_P/P}{\sigma_A/A} = \frac{\sigma_P}{P}\sqrt{A} = \frac{\sqrt{A}}{\sqrt{P}}\sqrt{1 + \left(1 + \frac{\eta_P}{\eta_B}\right)\left[\frac{B}{P}\right]} \qquad (30)$$

Equation (30) is simply equation (6), but with the additional factor under the large square root sign that expresses the degradation of precision caused by the statistical uncertainty in the background. Note that the degradation is sensitive to the peak-to-background ratio, P/B. As the peak-to-background ratio tends towards infinity, the degradation caused by the background tends towards zero. The degradation is somewhat less sensitive to the ratio of the peak and background window widths. A typical compromise is to choose $\eta_B = \eta_P$ so that the multiplier in parenthesis in front of B/P becomes 2. A wider background integration width, η_B, lowers the background degradation, but not by much.

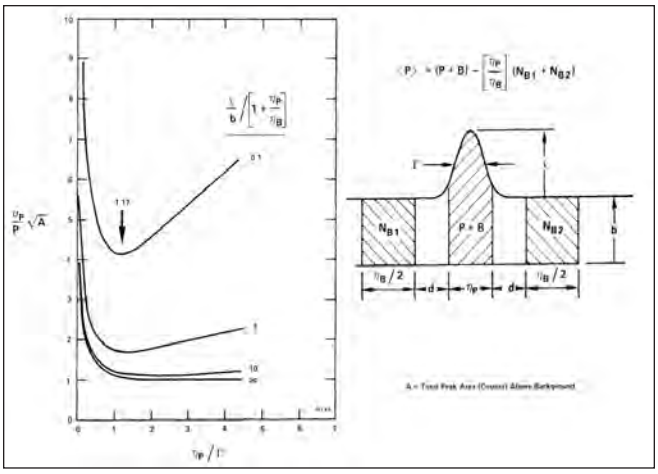

Figure 6. The dependence of the relative standard deviation in the net peak counts, σ_P/P, on the ratio of the peak amplitude, ℓ, to the background amplitude, b, and on the width of the integration regions. <P> is the estimate of the net peak counts obtained by subtracting the background estimate from the peak plus background counts.

Equation (30) is plotted in Figure 6 for a Gaussian peak of height ℓ and FWHM, Γ. The average amplitude of the background is b. This graph is the same as Figure 2, except the precision degradation due to the background has been added. The parameter, (ℓ/b)/[1 + (η_P/η_B)], that specifies each of the four curves in Figure 6 depends mildly on η_P/η_B and strongly on ℓ/b.

For clarification, consider a specific case of $\eta_P/\Gamma = 3$ and $\eta_P = \eta_B$. This makes it obvious that the ratio of the peak amplitude to the background height, ℓ/b, is proportional to the peak-to-background ratio, P/B. Consequently, the parameter defining the four curves is related to the peak-to-background ratio, P/B. If there is no background under the peak, then P/B = ∞ and ℓ/b = ∞. Thus, the bottom curve in Figure 6 is the case of zero background, and it is identical to the function plotted for zero background in Figure 2. Stepping vertically from the bottom curve (∞) to the next curve (10) adds a background, and establishes a finite peak-to-background ratio. Moving to the next curve (1) is equivalent to lowering the peak-to-background ratio by a factor of 10. The top curve (0.1) drops the peak-to-background ratio by another factor of 10. Note how increasing the background degrades the statistical precision in the net peak counts. The relative standard deviation in the net peak counts, σ_P/P, increases as the peak-to-background ratio decreases.

Figure 6 reveals another quirk caused by the background. For an infinite peak-to-background ratio (i.e., zero background) the minimum relative standard deviation in the net peak counts is obtained by using a peak integration window width that is more than twice the FWHM of the peak. However, at low peak-to-background ratios (0.1), the minimum relative standard deviation is achieved at $\eta_P = 1.17\ \Gamma$. This implies that the peak integration window width should be set at 1.17 times the FWHM of the peak to achieve the lowest detection limits. Such a narrow window makes the results extremely sensitive to a misalignment of the center of the peak integration window with respect to the centroid of the peak. Near detection limits, counting statistics obscures the shape of the peak, making it hard to center the integration window on the peak. Consequently, it is advisable to set the width of the peak integration window two to three times the FWHM of the peak. This choice minimizes the consequences of misalignment, while degrading the relative standard deviation by only 26%. (Compare $A^{1/2}\sigma_P/P$ at $\eta_P = 3\ \Gamma$ and $\eta_P = 1.17\ \Gamma$ on the 0.1 curve in Figure 6.) This is a very small price to pay for insulating the results from misalignment of the peak and window.

How Background Controls Detection Limits

Determining detection limits in the presence of background requires the use of statistical confidence limits. Confidence limits are most readily computed by using the Gaussian approximation to the Poisson distribution. Figure 7 illustrates a Gaussian probability distribution and defines the 5% and 95% confidence limits. The horizontal axis in Figure 7 utilizes a simplifying substitution in the exponent of equation (18).

$$z = \frac{N - \mu}{\sigma} \quad (31)$$

This substitution shifts the mean to zero, and expresses the deviation from the mean in units of the standard deviation, σ. This normalized Gaussian probability distribution has the form found in most statistical tables[2]:

$$G(z) = \frac{e^{-z^2/2}}{\sqrt{2\pi}} \quad (32)$$

The 5% confidence limit occurs at z = –1.6449. Because the area of the Gaussian to the left of this coordinate value is 5% of the total area, there is only a 5% probability of observing events to the left of z = –1.6449. Similarly, the 95% confidence limit occurs at z = +1.6449, because 95% of the area of the Gaussian distribution lies to the left of this value of z. In other words, there is a 95% probability of observing events with values of z to the left of z = +1.6449.

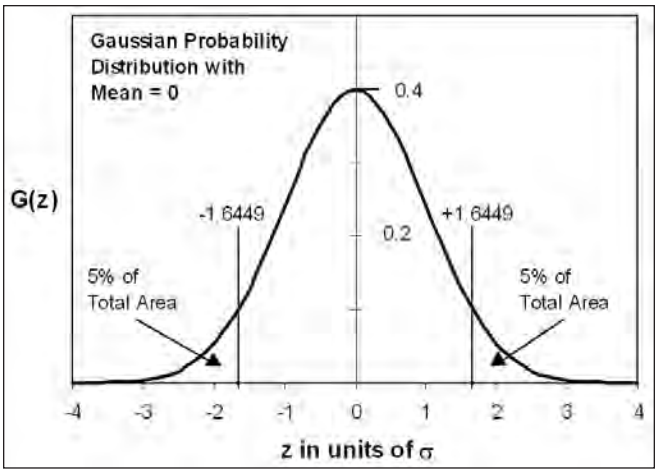

Figure 7. The Gaussian probability distribution and the definition of the 5% and 95% confidence limits.

Expressing these limits in terms of N via equation (31), the 5% and 95% confidence limits are

$$N_{5\%} = \mu - 1.6449\,\sigma \quad (33a)$$

$$N_{95\%} = \mu + 1.6449\,\sigma \quad (33b)$$

Caution must be exercised in applying the 5% and 95% confidence limits from a Gaussian distribution to the Poisson probability distribution at low values of μ, because the Poisson distribution is defined only at integer values of N, whereas the Gaussian distribution is continuous in N. Thus, the limits obtained from equation (33) must be rounded to the nearest integer value of N when applied to the Poisson distribution. To keep the rounding error less than 5% of 1.6449 σ, the value of μ must be ≥37. Normally, this is not a severe limitation.

For the calculation of the detection limit, the procedure illustrated in Figure 5 using equation (27) will be employed to measure the net peak counts. To claim detection, the net peak counts must exceed a threshold value set at N_D. The convention is to set this threshold high enough that there is only a 5% probability of the background counts exceeding the threshold if the peak truly is not present. This establishes the 5% false positive condition. From equation (29) , the standard deviation in the net peak counts when the net peak counts are zero is

$$\sigma_0 = \sqrt{\left(1 + \frac{\eta_P}{\eta_B}\right) B} \quad (34)$$

Therefore the threshold for a 5% false positive (95% true negative) is obtained from equation (33b).

$$N_D = \mu_0 + 1.6559\,\sigma_0 \approx 0 + 1.6449 \sqrt{\left(1 + \frac{\eta_P}{\eta_B}\right) B} \quad (35)$$

When the peak truly is present at the detection limit, P_{DL}, the conventional definition of the detection limit requires a 95% probability of claiming a true positive, and a 5% probability of a false negative. For this case the detection threshold, N_D, is determined by equations (33a) and (29).

$$N_D = \mu_P - 1.6449\,o_P \approx P_{DL} - 1.6449 \sqrt{P_{DL} + \left(1 + \frac{\eta_P}{\eta_B}\right) B} \quad (36)$$

Setting the detection thresholds equal between equations (35) and (36), and using the fact that P_{DL} « B to eliminate P_{DL} from the square root sign in equation (36) leads to the detection limit

$$P_{DL} \approx (2)(1.6449) \sqrt{\left(1 + \frac{\eta_P}{\eta_B}\right) B} \quad (37)$$

A more meaningful relationship can be obtained by expressing the detection limit in terms of concentration or activity, where the calibration equation relating concentration to net peak counts is

$$C = K\,P \quad (38a)$$

$$C_{DL} = K P_{DL} \qquad (38b)$$

C is the concentration or activity, and K is the calibration constant. C_{DL} is the detection limit in units of concentration. Substituting equations (38) in equation (37) produces

$$C_{DL} = \frac{3.29\, C\sqrt{\left(1+\frac{\eta_P}{\eta_B}\right)}}{\sqrt{\left(\frac{P}{B}\right)\left(\frac{P}{t}\right)t}} \qquad (39)$$

Equation (39) can be used to estimate the detection limit in the following way. A sample whose concentration C for the analyte is about a factor of 10 above the expected detection limit is measured. The net peak counts, P, the background counts, B, and the counting time, t, are noted and entered into equation (39) to calculate the predicted detection limit, C_{DL}.

More importantly, equation (39) reveals the factors that control detection limits. For a sample with a specific concentration, C, and a chosen value for η_P/η_B, the numerator of equation (39) is a constant. The denominator shows that the detection limit depends on

a) the peak-to-background ratio, P/B,
b) the net counting rate in the peak, P/t, and
c) the counting time, t.

Increase any one of these parameters by a factor of 4 and the detection limit will decrease by a factor of 2.

The most easily controlled parameter that influences the detection limit is the counting time, t. However, in most applications there is a limit to the counting time. If an improvement of a factor of 10 is needed in detection limits, and the counting time is already 1 day, 100 days would be needed. Such a long counting time is unlikely to be a viable option.

In some cases, the peak-to-background ratio can be increased by improving the spectrometer, or by pre-concentration of the analyte in the sample. Similar techniques can also be used to increase the net counting rate in the peak.

Conclusion

Clearly, it is important to maximize the peak-to-background ratio, the net counting rate in the peak, and the counting time to achieve the lowest detection limits. This same strategy is also important for achieving the best relative standard deviation for concentrations well above the detection limit.

References

1. Ron Jenkins, R. W. Gould, and Dale Gedcke, *Quantitative X-Ray Spectrometry*, Marcel Dekker, New York, First Edition (1981), pp 209 – 229.
2. Phillip R. Bevington, and D. Keith Robinson, *Data Reduction and Error Analysis for the Physical Sciences*, WCB McGraw-Hill, Boston, Second Edition, (1992).
3. Ibid. ref. 1, pp 229 – 244 and 252 – 276.
4. *1997/1998 EG&G ORTEC Catalog*, pp 2.176 – 2.178
5. *ORTEC Modular Pulse Processing Electronics Catalog (2001)*, Oak Ridge, USA, pp 8.3 – 8.4
6. Ibid. ref. 4, pp 2.282 – 2.283.
7. Ibid. ref. 5, pp 10.6 – 10.7.
8. D.A. Gedcke, ORTEC Application Note AN57, *Dealing with Dead Time Distortion in a Time Digitizer*, (2001).
9. D. A.Gedcke, ORTEC Application Note AN58, *How Histogramming and Counting Statistics Affect Peak Position Precision*, (2001).
10. Ibid. ref. 1, pp 337 – 360.
11. Robert L. Coldwell and Gary J. Bamford, *The Theory and Operation of Spectral Analysis Using ROBFIT*, American Institute of Physics, New York, 1991.
12. Ronald M. Keyser, Nucl. Instr. and Meth. A286 (1990) pp 403 – 414.
13. John D. Valentine and Asad E. Rana, *Centroid and Full-Width at Half Maximum Uncertainties of Histogrammed Data with an Underlying Gaussian Distribution — The Moments Method*, IEEE Trans. Nucl. Sci. Vol. 43, No. 5, Oct. 1996, pp 2501 – 2508.

Specifications subject to change
070809

ORTEC®
www.ortec-online.com
Tel. (865) 482-4411 • Fax (865) 483-0396 • ortec.info@ametek.com
801 South Illinois Ave., Oak Ridge, TN 37831-0895 U.S.A.
For International Office Locations, Visit Our Website
AMETEK®
ADVANCED MEASUREMENT TECHNOLOGY